

Paper:

# Simulation of Tsunami Inundation in Central Peru from Future Megathrust Earthquake Scenarios

Erick Mas<sup>\*1</sup>, Bruno Adriano<sup>\*2</sup>, Nelson Pulido<sup>\*3</sup>, Cesar Jimenez<sup>\*4</sup>, Shunichi Koshimura<sup>\*1</sup>

<sup>\*1</sup>Laboratory of Remote Sensing and Geoinformatics for Disaster Management  
International Research Institute of Disaster Science, Tohoku University  
Aoba 468-1, Aramaki, Aoba-ku, Sendai, Miyagi, Japan  
E-mail: mas@irides.tohoku.ac.jp

<sup>\*2</sup>Graduate School of Engineering, Tohoku University, Miyagi, Japan

<sup>\*3</sup>National Research Institute for Earth Science and Disaster Prevention (NIED), Ibaraki, Japan

<sup>\*4</sup>Universidad Nacional Mayor de San Marcos Fenlab., Lima, Peru

[Received July 1, 2014; accepted September 19, 2014]

We estimated, from twelve scenarios of potential megathrust earthquakes, the tsunami impact on the Lima-Callao region in Central Peru. In addition, we conducted hazard mapping using the local envelope of the maximum inundation simulated in these scenarios. The deterministic approach is supported by the decades of geodetic measurements in this area that characterize the interseismic strain build up since historical megathrust earthquakes. The earthquake scenarios for simulation proposed in [1] introduce spatially correlated short-wavelength slip heterogeneities to a first slip model in [2] calculated from the interseismic coupling (ISC) distribution in Central Peru. The ISC was derived from GPS monitoring data as well as from historical earthquake information. The results of strong ground motion simulations in [1] reported that the slip scenario with the deepest average peak values along the strike ( $M_w = 8.86$ ) generates the largest PGA in the Lima-Callao area. In this study, we found from tsunami simulation results that the slip model with the largest peak slip at a shallow depth ( $M_w = 8.87$ ) yielded the highest tsunami inundation. Such differences in maximum scenarios for peak ground acceleration and tsunami height reveal the importance of a comprehensive assessment of earthquake and tsunami hazards in order to provide plausible worst-case scenarios for disaster risk management and education.

**Keywords:** tsunami simulation, megathrust earthquake, tsunami hazard, Peru

## 1. Introduction

Megathrust earthquakes are extremely large thrust fault earthquakes, thrust being the upward movement of one side of a fault relative to the other. Megathrust earthquakes, which occurred at plate interfaces along subduction zones, present magnitudes over  $M_w 8.5$  and

are especially destructive when over  $M_w 9.0$ . Such events have caused great number of casualties in the past. In the last decade, the 2004 Sumatra ( $M_w 9.2$ ), 2010 Chile ( $M_w 8.8$ ) and 2011 Japan ( $M_w 9.0$ ) events have highlighted the importance of assessing extreme scenarios of strong ground motion and tsunami impact. Our study area is in the Central coast of Peru facing the Peru-Chile trench, where the subduction of the Nazca Plate under the South American Plate is responsible for earthquakes of magnitudes ( $M_w$ ) greater than 8.2 approximately every 25 years [3, 4]. In addition, in Central Peru, the built up areas of the capital city of Lima and the national port of Callao are located near the coast. Huge earthquakes triggering tsunami events have occurred in the past and have been recorded at least since the era of the Spanish occupation of the Inca empire in the 16<sup>th</sup> century. Nowadays, the potential damage to the national infrastructure exposed in Callao and Lima could yield not only a large number of casualties and damage but also a dramatic breakdown in the Peruvian economy. Thus, the risk of destructive earthquakes and tsunamis is high and must be addressed by disaster managers.

Accordingly, this paper studies the area of seismic gap and accumulated stress that correspond to the rupture area of the 1746 megathrust earthquake. Here, building on the shoulders of previous seismological research [1, 2, 5–7], we perform tsunami simulations for twelve megathrust earthquake scenarios in order to grasp the tsunami hazard of a potential future disaster. The outcomes of the tsunami inundation simulations are merged with a point by point maximum depth envelope to form a deterministic-based hazard map to be proposed for disaster education and mitigation in Central Peru.

## 2. Background

### 2.1. Megathrust Earthquakes in Peru

The rapid convergence of the oceanic Nazca Plate with the South American Plate ( $60 - 70 \text{ mm yr}^{-1}$ ) has produced large subduction earthquakes listed in several

catalogues and research papers of historical events in Peru [3, 4, 8–12]. The largest earthquake to occur in Central Peru so far has been the October 28, 1746 event. Its magnitude has been estimated to have been from  $M_w$ 8.6 [5, 9, 13] to even  $M_w$ 9.0 [14]. The 1746 Lima-Callao earthquake claimed 5,941 lives. In central Lima 1,141 people were killed by the strong motion, and in Callao only 221 out of the 5,000 inhabitants survived the tsunami [15–17]. Surprisingly, in a recent paleotsunami study conducted by Spiske et al. [4], no trace of the 1746 tsunami was found in the areas sampled along the coast of Peru, possibly due to urban sprawl or eolian processes that have disturbed tsunami sediments (Spiske, personal communication, 2014).

During the 18<sup>th</sup> and 19<sup>th</sup> centuries large megathrust earthquakes and tsunamis were triggered north of the Nazca Ridge, in 1746, and south of it, in 1868. It has long been suggested that the Nazca Ridge may act as a barrier to the rupture propagation of earthquakes in Central Peru [12, 18]. Similarly, the north edge of the 1746 rupture area is bordered with the Mendaña fracture zone (FZ), another possible natural boundary for Central Peru earthquake rupture propagation. Consequently, it is believed that the 1746 earthquake rupture area propagated from approximately the Mendaña FZ to the Nazca Ridge (> 500 km). Within this area, four large earthquakes have occurred with  $M_w$ 8.0 in 1940, 1966, 1974 and 2007, representing only a 23% of the moment deficit accumulated since 1746. Thus, a significant amount of seismic moment is still to be released in Central Peru [5].

**2.2. Previous Studies and Data for Simulation**

Chlieh et al. [5] have derived, from two decades of geodetic measurements in Peru and Chile, the interseismic strain build up along the subduction zone from Lima, Peru to Antofagasta, Chile (Fig. 1). The areas of high seismic slip agreed with the portions of high inter seismic coupling (ISC), proving effective the assessment of location, size, and magnitude of future large megathrust earthquakes in subduction zones. In the case of Central Peru, the area ruptured after 1746 ( $M_w$ 8.6-8.8) released some of the elastic strain built up to the moment. However, it resulted in a small amount of the expected accumulated elastic strain [5]. Thus, it is possible for a megathrust earthquake of magnitude  $M_w > 8.5$  to occur in this area of high ISC (Fig. 1).

Based on this model of ISC distribution, two areas strongly coupled are off the coasts of the cities of Lima and Pisco (Fig. 1). Assuming the interseismic period of 265 years from the last megathrust earthquake in 1746 to 2010, Pulido et al. [2] obtained a slip deficit model equivalent to a magnitude  $M_w$ 8.9 earthquake (Fig. 2). The tsunami impact of this source model was studied by Adriano et al. [7].

In addition, for strong motion simulations it was necessary to add short wavelength heterogeneities to the source slip to simulate high frequency ground motions: long wavelength asperities were already present within the original megathrust model. Subsequently, Pulido et

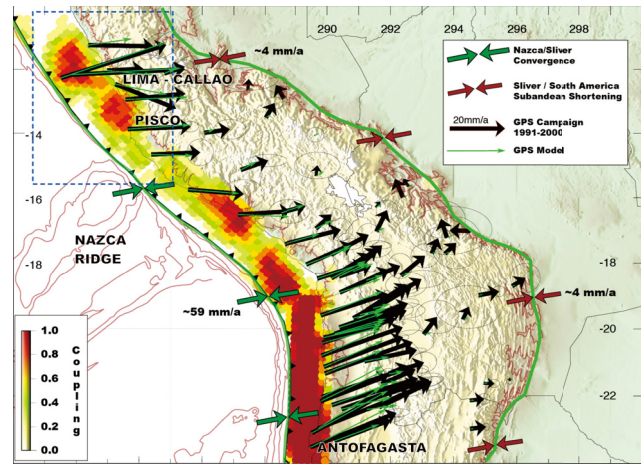


**Fig. 1.** Interseismic Coupling (ISC). Distribution of asperities and regional accumulated stress reported by [5]. The rectangular inset corresponds to the Lima-Callao area in Central Peru.

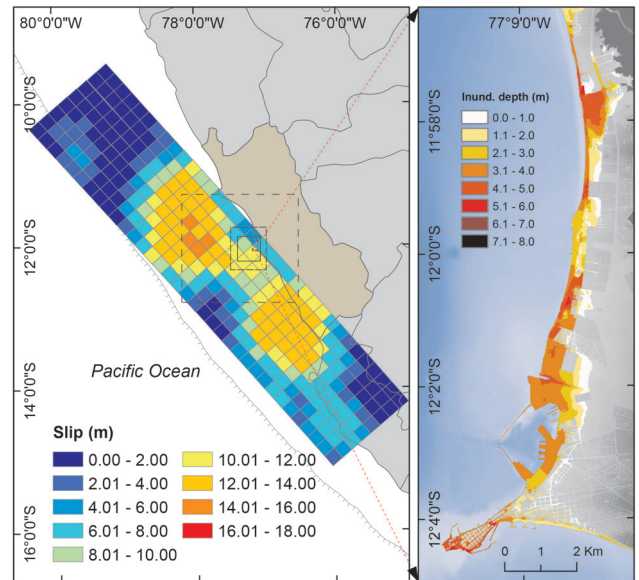


**Fig. 2.** Slip Deficit Model and Domains for tsunami simulation. The slip deficit model developed by [2] (left) and tsunami simulation result reported in [7] (right). In this study, we used the same nested grid domains to simulate the 12 megathrust earthquake scenarios shown in Fig. 3.

al. [1] calculated twelve different slip distributions from the original slip deficit source by combining the geodetic slip model (GSM) with several short wavelength slip distributions. Details of the strong motion simulation can be found in [6]<sup>1</sup>. Fig. 3 shows the 12 mega-earthquake scenarios. Strong motion simulation results in [6] suggest that the slip with the deepest average peak value along the strike (Model 5) generates the largest PGA in Lima-Callao ( $\approx 1000 \text{ cm/s}^2$ ). Consequently, to grasp the tsunami risk posed by such mega-earthquakes in

1. For the 12 slip deficit models, the original source of Fig. 2 was reduced in length. Patches on the north and south edges with small slip values were eliminated.

**Table 1.** Source parameters of 12 megathrust earthquake sources [1] used for tsunami modeling in this study and the maximum inundation depth resulting from simulation.

Model	Lon (deg)*	Lat (deg)*	Depth*	Slip (m)*	Rake (deg)	Strike (deg)	Dip (deg)	Width (km)	Length (km)	Max. Inund. Depth (m)
1	-77.80	-11.88	32.03	17.61	55.70	319.00	15.00	480.00	160.00	6.87
2	-78.30	-11.58	26.85	17.86	55.70	319.00	15.00	480.00	160.00	7.82
3	-78.31	-11.83	21.68	17.30	55.70	319.00	15.00	480.00	160.00	6.46
4	-78.32	-11.96	19.09	19.92	55.70	319.00	15.00	480.00	160.00	7.98
5	-78.04	-11.48	34.62	18.24	55.70	319.00	15.00	480.00	160.00	6.09
6	-78.08	-12.23	19.09	18.86	55.70	319.00	15.00	480.00	160.00	7.55
7	-76.43	-13.57	29.44	17.32	55.70	319.00	15.00	480.00	160.00	6.93
8	-77.86	-11.81	32.03	15.64	55.70	319.00	15.00	480.00	160.00	6.21
9	-78.00	-11.92	26.85	16.85	55.70	319.00	15.00	480.00	160.00	7.00
10	-76.86	-13.35	24.26	15.66	55.70	319.00	15.00	480.00	160.00	6.15
11	-78.00	-12.05	24.26	16.32	55.70	319.00	15.00	480.00	160.00	7.86
12	-76.54	-13.31	32.03	16.50	55.70	319.00	15.00	480.00	160.00	6.59

\*These data correspond to the subfault with the maximum slip.

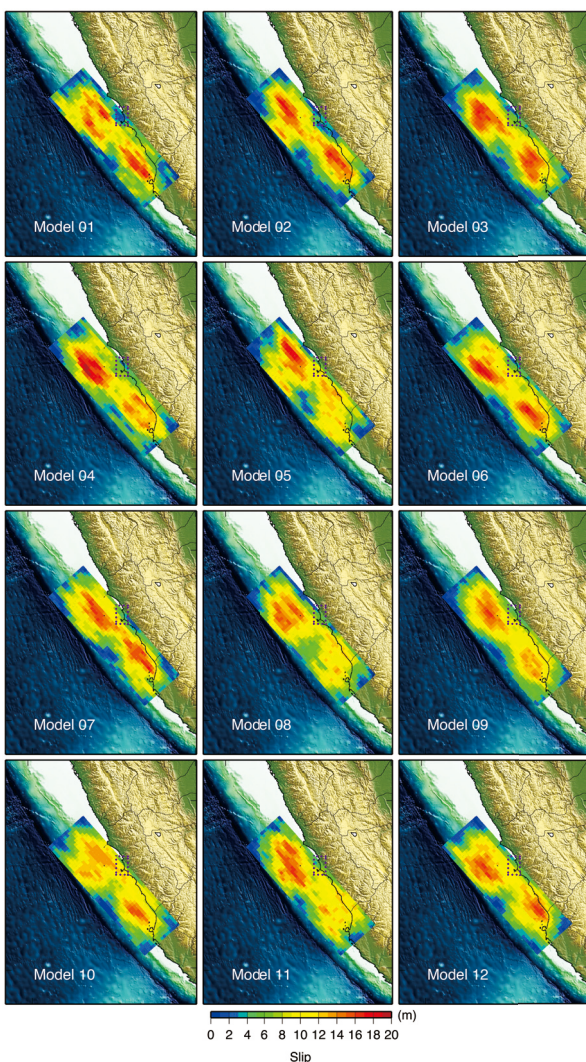


**Fig. 3.** Mega-earthquake scenarios. Slip distribution for 12 scenarios of slip deficit in Central Peru [19]. The small rectangle shows the area of study for the tsunami simulations.

Lima-Callao, we evaluate the tsunami impact and the differences in the spatial features of slip sources as they relate to tsunami inundation.

### 3. Tsunami Numerical Modeling

In this study, the Tohoku University Numerical Analysis Model for Investigation of Near-field tsunami No.2 (TUNAMI-N2) was used for the simulation. Nonlinear shallow water equations were discretized using a staggered leap-frog finite difference scheme [20]. The computational region was divided into five domains represented by nested grids, as seen in the rectangular insets in **Fig. 2**. The bathymetry data was originally obtained from GEBCO<sup>2</sup> at a 30 arc-sec resolution and was resampled for the first and second domains into 405 m and 135 m, respectively. In the case of the third to fifth domains, nautical charts and echo sounder bathymetry data were provided by DHN<sup>3</sup> from a 2014 new bathymetry acquisition campaign in the area. Topography data was obtained from the Regional Government of Callao as contour lines. A 5 m grid resolution was used in the smallest domain of simulation. In general, detailed digital urban information, such as building outlines and building heights, were limited in this area. In addition, building heights could not be included as part of a topographic model, except for a small district located in the peninsula called La Punta, where data on building heights were included in the topography. An instantaneous displacement of the sea surface, identical to the vertical sea floor displacement, is assumed in the tsunami source model by means of the Okada's analytical formula for the static deformation of elastic half-space induced by a uniform co-seismic slip on rectangular faults [21]. Each scenario of slip deficit consists of 768 subfaults of 10 × 10 km located offshore from Lima. **Table 1** shows the source parameters of the twelve megathrust earthquake scenarios for numerical tsunami simulation. Due to the large number of subfaults per model, parameters shown in the table were limited to the subfault with maximum slip value. A total of 3 hours of computation time was set for each model with a time step of 0.1 s. Inundation was calculated for the smallest

2. General Bathymetric Chart of the Oceans. ([www.gebco.net](http://www.gebco.net))

3. Direccion de Hidrografia y Navegacion de la Marina de Guerra del Peru

domain using a 5 m grid size domain with building height information included in the topography (topographic model) for the area of La Punta, the peninsula of Lima-Callao. For other areas and domains, a constant Manning roughness value of 0.025 was used.

#### 4. Results and Discussion

The outputs of the numerical tsunami simulations of the 12 mega-earthquake scenarios are shown in **Fig. 4**. In addition, the maximum inundation depth resulting from each model simulation is shown in the right column of **Table 1**.

Results show that the area of inundation does not vary significantly (**Fig. 4**), and the local maximum inundation depth can differ up to 1.9 m across the scenarios (**Table 1**). In addition, according to [1, 6], Model 5 is the scenario with the maximum values in strong motion for Lima-Callao. However, it yields a lower run-up, depth, and area of inundation ( $\approx 16.3 \text{ km}^2$ ) than does Model 4, which has the overall maximum run-up, depth, and area of inundation ( $\approx 18.4 \text{ km}^2$ ). Such differences in the worst-case scenario for strong motion simulation and tsunami simulation may be explained by the spatial distribution and values of maximum slip from each source. For example, in **Table 1**, we can observe that Model 5 presents the third highest slip value (18.24 m), after Model 4 (19.92 m) and Model 6 (18.86 m), but it has a much greater maximum slip depth than do the other models (34.62 m). These spatial distribution and maximum slip values can also be confirmed in **Fig. 3**. Therefore, it is observed that the source with the deepest along-strike slip, which is at the same time closer to the coast of Central Peru, results in the strongest ground motion in the study area, as suggested before by [1]. This condition is enhanced if the rupture nucleation point is in the shallow area with directivity towards Lima. Conversely, Model 4, the worst-case scenario of tsunami inundation, is triggered by the model with the largest peak slip in a shallow region. It is important for such differences in the worst case scenarios for strong ground motion and tsunami inundation to be noticed and communicated to the layperson for their disaster prevention education, since tsunami awareness and self-evacuation behavior in areas such as Peru and Chile are based mostly on people’s own risk perception triggered by the earthquake intensity [22]. There is a local saying in these coastal areas that “the first warning is the earthquake itself, and whenever you cannot stand up during an earthquake, a tsunami might soon follow.” While this statement does not lack truth, it can result in dangerous behavior when, for example, tsunami-earthquakes occur [13, 23], since, as shown in this paper, although it is a non tsunami-earthquake mechanism, the strongest motion (Model 5,  $\text{PGA} > 1000 \text{ cm/s}^2$ , Max. Inund.  $\approx 6 \text{ m}$ ) does not yield the highest tsunami inundation (Model 4,  $\text{PGA} < 500 \text{ cm/s}^2$ , Max. Inund.  $\approx 8 \text{ m}$ ).

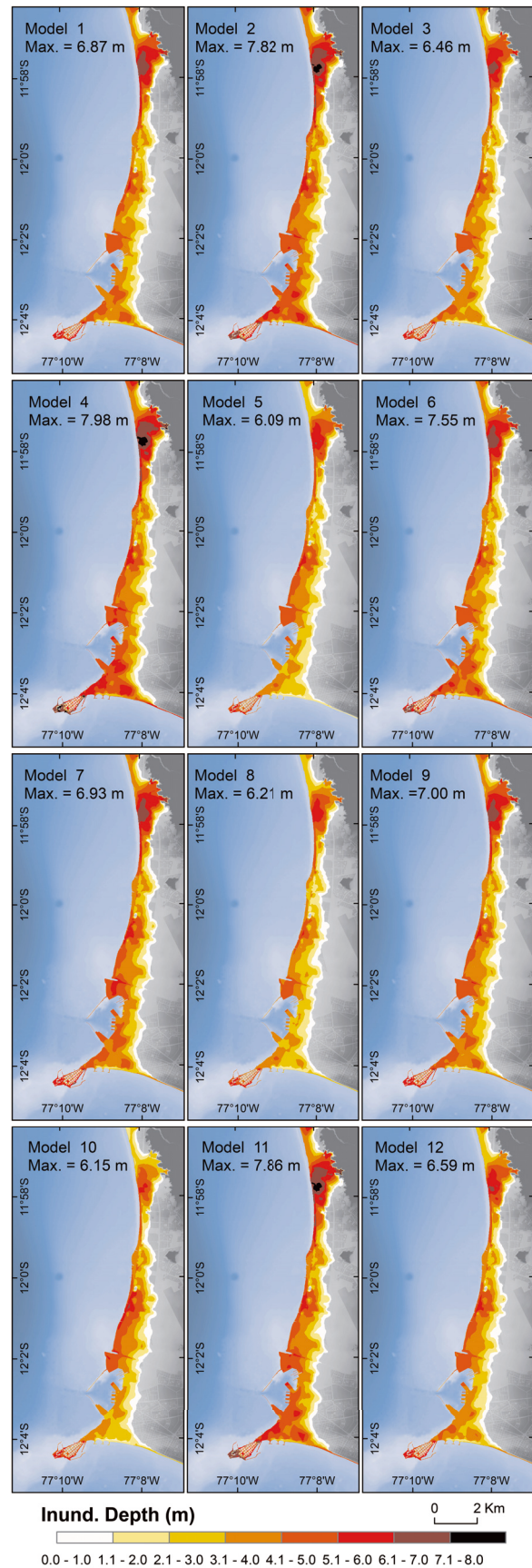


**Fig. 4.** Tsunami Inundation results. Tsunami inundation in 12 mega-earthquake scenarios in Central Peru. The maximum value corresponds to the maximum inundation depth within the entire study area. Model 4 results in the highest level of tsunami hazard.

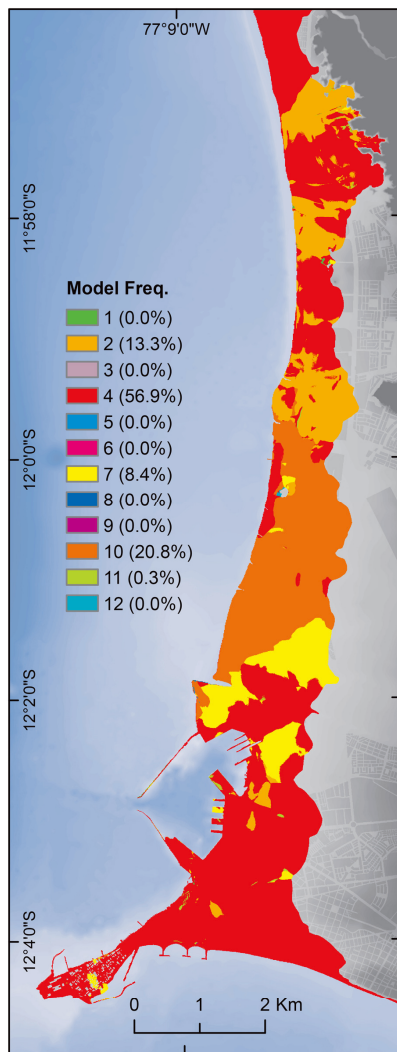


**Fig. 5.** Model frequency. Spatial distribution of maximum inundation at each point from the output of the comparison of 12 models. The percentage denotes the frequency of presence from the model in the plot, based on the number of grids per model with respect to the total number of grids in the envelope.

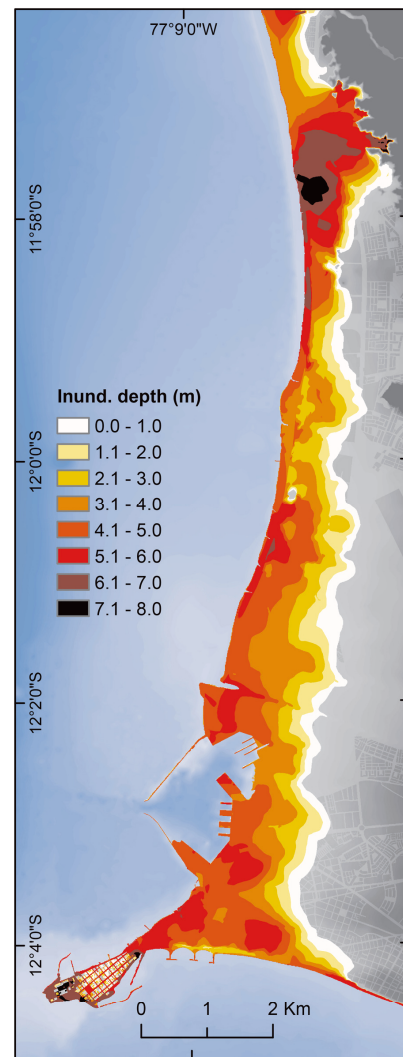


**Fig. 6.** Maximum of the maximum inundation from 12 scenarios. An envelope of inundation depths showing the maximum value of the outputs from the 12 models at each grid cell.

## 5. Hazard Mapping

A previous hazard mapping effort was conducted by [7] using local bathymetry data lower in resolution and accuracy than the data gathered in 2014 in a new bathymetry campaign by DHN-Peru for this study. In addition, the topographic model presented in [7] assumes a height of two-stories at a block scale for buildings in the entire computational domain, including areas where no building height data was available. Due to the high uncertainty of the potential tsunami damage to buildings, as suggested by [24], we decided to avoid this assumption that yields lower areas and depths of inundation and prepare hazard maps with constant roughness model results. Simulations of the tsunami inundation resulting from future megathrust earthquake scenarios in Central Peru show areas at risk of inundations approximately

6 m to 8 m deep. The maximum inundation depth and inundated area was found to be that in Model 4, which presents the maximum slip value. However, there is a small correlation between maximum slip and maximum tsunami height in these scenarios ( $r = 0.53$ ,  $R^2 = 0.28$ ) and in general [25]. Therefore, instead of relying only on Model 4 as the worst-case scenario for disaster mitigation activities, another approach would be to use the maximum local inundation depth at each grid cell of the study area from all scenarios. **Fig. 5** illustrates the spatial distribution of maximum inundation depths at each point in the 12 model results with their corresponding frequency calculated by the percentage of grids from each model with respect to the total number of grids in the envelope of tsunami inundation. Consequently, 57% of grids in the inundation envelope correspond to Model 4 tsunami numerical simulation results, while 21% and 13% correspond to Model 10 and Model 2, respectively. Thus, we propose **Fig. 6** as a tsunami hazard map for

short and mid-term tsunami disaster mitigation activities in the study area.

## 6. Conclusions

We have conducted the tsunami inundation simulation of 12 mega-earthquake scenarios in Central Peru to propose a short to mid-term tsunami hazard map useful for tsunami mitigation activities in the study area of Lima-Callao, Peru. In addition, worst-case scenarios for strong ground motion and tsunami inundation simulations resulted from different settings of slip deficit models. While the strongest motion is generated by the slip distribution where the highest value is in the deep region and closer to the study area the highest tsunami inundation is generated by the slip distribution with the largest peak slip value in a shallower area. Therefore, the earthquake intensity expected from the worst-case scenario of tsunami inundation is not necessarily the maximum intensity produced by the worst-case scenario of strong motion. Since residents' evacuation behavior in these regions relies on cues from earthquake intensities, it is important to educate the population as to the possibility of smaller intensities and higher tsunami inundations, such as the case studied here, or to the possibility of tsunami-earthquakes on the Peruvian coast.

## Acknowledgements

This study was carried out under the framework of the SATREPS project Enhancement of Earthquake and Tsunami Disaster Mitigation Technology in Peru, sponsored by the Japan International Cooperation Agency (JICA) and the Japan Science and Technology Agency (JST). Our appreciation goes to the Ministry of Education, Culture, Sports, Science, and Technology (MEXT); Tohoku University; the National Research Institute for Earth Science and Disaster Prevention (NIED), and the International Research Institute of Disaster Science (IRIDeS) for their support. We would like to thank Dr. Mohamed Chlieh for his support and for kindly providing the map included as **Fig. 1** in this paper.

## References:

- [1] N. Pulido, H. Tavera, Z. Aguilar, D. Calderon, M. Chlieh, T. Sekiguchi, S. Nakai, and F. Yamazaki, "Mega-earthquakes rupture scenarios and strong motion simulations for Lima, Peru," in *The International Symposium for CISMID 25<sup>th</sup> Anniversary*, pp. 1-8, 2012.
- [2] N. Pulido, H. Tavera, H. Perfettini, M. Chlieh, Z. Aguilar, S. Aoi, S. Nakai, and F. Yamazaki, "Estimation of Slip Scenarios for Megathrust Earthquakes: A Case Study for Peru," in *4<sup>th</sup> IASPEI/IAEE International Symposium*, (Santa Barbara, CA, USA), pp. 1-6, 2011.
- [3] P. Lockridge, "Tsunamis in Peru-Chile," *Tech. Rep. July*, National Geophysical Data Center, 1985.
- [4] M. Spiske, J. Piepenbreier, C. Benavente, A. Kunz, H. Bahlburg, and J. Steffahn, "Historical tsunami deposits in Peru: Sedimentology, inverse modeling and optically stimulated luminescence dating," *Quaternary International*, Vol.305, pp. 31-44, Aug. 2013.
- [5] M. Chlieh, H. Perfettini, H. Tavera, J.-P. Avouac, D. Remy, J.-M. Nocquet, F. Rolandone, F. Bondoux, G. Gabalda, and S. Bonvalot, "Interseismic coupling and seismic potential along the Central Andes subduction zone," *Journal of Geophysical Research*, Vol.116, pp. 1-21, Dec. 2011.
- [6] N. Pulido, Z. Aguilar, H. Tavera, M. Chlieh, D. Calderón, T. Sekiguchi, S. Nakai, and F. Yamazaki, "Source models scenarios and strong ground motion for future mega-earthquakes: Application to Lima, Central Peru," *Bulletin of the Seismological Society of America* (in review).
- [7] B. Adriano, E. Mas, S. Koshimura, Y. Fujii, S. Yauri, C. Jimenez, and H. Yanagisawa, "Tsunami Inundation Mapping in Lima , for Two Tsunami Source Scenarios," *Journal of Disaster Research*, Vol.8, No.2, pp. 274-284, 2013.
- [8] W. H. Berninghausen, "Tsunamis reported from the West coast of South America," *Bulletin of the Seismological Society of America*, Vol.52, No.4, pp. 915-921, 1962.
- [9] L. Dorbath, A. Cisternas, and C. Dorbath, "Assessment of the size of large and great historical earthquakes in peru," *Bulletin of the Seismological Society of America*, Vol.80, No.3, pp. 551-576, 1990.
- [10] J. Carpio and H. Tavera, "Estructura de un Catalogo de Tsunamis para el Peru. Basado en el Catalogo de Gusiakov (2002)," *Boletin de la Sociedad Geologica del Peru*, Vol.94, pp. 45-59, 2002.
- [11] E. A. Kulikov, A. B. Rabinovich, and R. E. Thomson, "Estimation of Tsunami Risk for the Coasts of Peru and Northern Chile," *Natural Hazards*, Vol.35, pp. 185-209, June 2005.
- [12] E. A. Okal, J. C. Borrero, and C. E. Synolakis, "Evaluation of Tsunami Risk from Regional Earthquakes at Pisco, Peru," *Bulletin of the Seismological Society of America*, Vol.96, pp. 1634-1648, Oct. 2006.
- [13] J.-M. Nocquet, M. Chlieh, P. Mothes, F. Rolandone, P. Jarrin, D. Cisneros, A. Alvarado, L. Audin, F. Bondoux, X. Martin, Y. Font, M. Régnier, M. Vallée, T. Tran, C. Beauval, J. M. n. Mendoza, W. Martinez, H. Tavera, and H. Yepes, "Motion of continental slivers and creeping subduction in the northern Andes," *Nature Geoscience*, Vol.7, pp. 1-5, April, 2014.
- [14] C. Jimenez, N. Moggiano, E. Mas, B. Adriano, S. Koshimura, Y. Fujii, and H. Yanagisawa, "Seismic Source of 1746 Callao Earthquake from Tsunami Numerical Modeling," *Journal of Disaster Research*, Vol.8, No.2, pp. 266-273, 2013.
- [15] J. Kuroiwa Horiuchi, "Disaster Reduction. Living in harmony with nature," *Editorial NSG*, first edit, ed., 2004.
- [16] P. E. Pérez-Mallaína, "Las catástrofes naturales como instrumento de observación social : el caso del terremoto de Lima en 1746," *Anuario de Estudios Americanos*, Vol.62, No.2, pp. 47-76, 2005.
- [17] E. Mas, B. Adriano, J. Kuroiwa Horiuchi, and S. Koshimura, "Reconstruction process and social issues after the 1746 earthquake and tsunami in Peru: past and present challenges after tsunami events," in V. Santiago-Fandino, Y. A. Kontar, and Y. Kaneda (Eds.), "Post-Tsunami Hazard Reconstruction and Restoration," pp. 1-18, Springer Netherlands, 2014 (in press).
- [18] H. Perfettini, J.-P. Avouac, H. Tavera, A. Kositsky, J.-M. Nocquet, F. Bondoux, M. Chlieh, A. Sladen, L. Audin, D. L. Farber, and P. Soler, "Seismic and aseismic slip on the central Peru megathrust," *Nature*, Vol.465, pp. 78-81, May 2010.
- [19] N. Pulido, Y. Yagi, H. Kumagai, and N. Nishimura, "Rupture process and coseismic deformations of the 27 February 2010 Maule earthquake, Chile," *Earth, Planets and Space*, Vol.63, pp. 955-959, Dec. 2011.
- [20] F. Imamura, "Review of tsunami simulation with a finite difference method," in H. Yeh, P. Liu, and C. E. Synolakis (Eds.), "Long-Wave Runup Models," pp. 25-42, Singapore: World Scientific Publishing Co., 1996.
- [21] Y. Okada, "Internal deformation due to shear and tensile faults in a half-space," *Bulletin of the Seismological Society of America*, Vol.82, No.2, pp. 1018-1040, 1992.
- [22] A. Marín, S. Gelcich, G. Araya, G. Olea, M. Espíndola, and J. C. Castilla, "The 2010 tsunami in Chile: Devastation and survival of coastal small-scale fishing communities," *Marine Policy*, Vol.34, pp. 1381-1384, Nov. 2010.
- [23] S. L. Bilek, "Invited review paper : Seismicity along the South American subduction zone: Review of large earthquakes, tsunamis, and subduction zone complexity," *Tectonophysics*, Vol.495, No.1-2, pp. 2-14, 2010.
- [24] A. Muhari, F. Imamura, S. Koshimura, and J. Post, "Examination of three practical run-up models for assessing tsunami impact on highly populated areas," *Natural Hazards and Earth System Science*, Vol.11, pp. 3107-3123, Dec. 2011.
- [25] V. K. Gusiakov, "Relationship of Tsunami Intensity to Source Earthquake Magnitude as Retrieved from Historical Data," *Pure and Applied Geophysics*, Vol.168, pp. 2033-2041, Mar. 2011.



**Name:**

Erick Mas Samanez

**Affiliation:**

Assistant Professor, Laboratory of Remote Sensing and Geoinformatics for Disaster Management (ReGiD), International Research Institute of Disaster Science (IRIDeS), Tohoku University

**Address:**

Aoba 468-1, Aramaki, Aoba-ku, Sendai, Miyagi, Japan

**Brief Career:**

1999-2004 B.S. Civil Engineering, National University of Engineering, Perú

2006-2009 M.Sc. Disaster Risk Management, National University of Engineering, Perú

2009-2012 Ph.D. Civil Engineering, Tsunami Engineering, Tohoku University, Japan

2012- Assistant Professor, ReGiD, IRIDeS, Tohoku University, Japan

**Selected Publications:**

• E. Mas, B. Adriano, S. Koshimura, F. Imamura, H. J. Kuroiwa, F. Yamazaki, C. Zavala, M. Estrada, "Identifying Evacuee's Demand of Tsunami Shelters using Agent Based Simulation," Published on "Tsunami Events and Lessons Learned," Y. Kontar, V. Santiago-Fandino, T. Takahashi (Eds.), Springer Netherlands, 2014.

• E. Mas, A. Suppasri, F. Imamura, and S. Koshimura, "Agent Based simulation of the 2011 Great East Japan Earthquake Tsunami evacuation. An integrated model of tsunami inundation and evacuation," Journal of Natural Disaster Science, Vol.34, Issue 1, pp. 41-57, 2012.

**Academic Societies & Scientific Organizations:**

- Peruvian Engineering College
  - Japan Society of Civil Engineers (JSCE)
  - Japan Geoscience Union (JpGU)
  - American Geophysical Union (AGU)
  - European Geosciences Union (EGU)
-